27th International Congress on Sound and Vibration
The annual congress of the International Institute of Acoustics and Vibration (IIAV)
11-16 July, 2021
ICSV27
Annual Congress of the International Institute of Acoustics and Vibration (IIAV)

# A GREEN'S FUNCTION APPROACH TO STUDY THERMO-ACOUSTIC INSTABILITIES IN THE PRESENCE OF NOISE

Sadaf Arabi
*School of Physical and Chemical Sciences, Keele University, Staffordshire ST5 5BG, United Kingdom*
*email: s.arabi@keele.ac.uk*

Maria Heckl
*School of Physical and Chemical Sciences, Keele University, Staffordshire ST5 5BG, United Kingdom*
*e-mail: m.a.heckl@keele.ac.uk*

Thermoacoustic instabilities are a major problem in combustion systems. In order to gain physical insight into thermoacoustic instabilities and to perform parameter studies, a fast analytical tool is invaluable. A Green's function approach provides such a tool. The most important advantage of the Green's function approach is the ability to alter boundary conditions, the heat release rate model, and also to impose noise from an external source. The Green's function approach can be combined with an amplitude-dependent model for the heat release rate, and then it allows us to predict nonlinear phenomena e.g. limit cycle, triggering, or hysteresis. In this paper, we adopt a Green's function approach for a specific geometry (Rijke tube). The nonlinear heat release rate model will be defined and the time-history of an evolving thermoacoustic instability will be calculated. Furthermore, we will investigate the effect of external noise on the time evolution of the acoustic field in the combustion system. We will calculate stability maps, focusing on heat source position as bifurcation parameter. At first, we will consider just one forcing term (heat release rate). Then, we will extend our formulation by adding a second forcing term to simulate the effect of random noise. The effect of the noise on the stability behaviour will be discussed.

Keywords: Thermoacoustic instabilities, Green's function, Rijke tube, Random noise

## 1. Introduction

Thermoacoustic instabilities can arise in systems consisting of an acoustic resonator and an unsteady heat source, e.g. a combustion chamber; they are due to a feedback between the acoustic field the heat release rate. Indeed, a small perturbation of the acoustic field can increase the heat release rate, which in turn can increase the acoustic field. The Green's function approach is a powerful mathematical tool to study instabilities in combustion systems. This analytical approach is a faster tool to predict the stability of combustion systems compared to numerical methods

One of the first to model nonlinear aspects of thermoacoustic instabilities with a Green's function approach was Heckl [1], who simulated Noiray's test rig [2]. This is a quarter-wave resonator with a matrix flame. Noiray measured the flame transfer function (FTF) of this flame for different excitation amplitudes and thus described the heat release rate by a flame describing function (FDF). Heckl modelled this FDF by an extended time-lag law, with amplitude-dependent $n$ (coupling coefficient) and amplitude-dependent $\tau$ (time-lag). Her stability predictions agreed well with some of Noiray's observations, but not with others. The FDF model was improved by Bigongiari and Heckl [3] and incorporated again in a Green's function approach. Their study successfully predicted the nonlinear phenomena of limit cycle, bistability, hysteresis, and frequency shift. The literature about noise in thermoacoustic systems is very limited. Among them, Jegadeesan and Sujith [4] performed an experimental study to investigate the effect of noise on stability of thermoacoustic systems. They observed noise induced triggering (NIT) which is the phenomenon of inducing an instability by adding noise to a previously stable system.

In this paper, we will use a Green's function approach to study the effects of random noise on the stability of a Rijke tube with length $L$ and an interface separating a cold region (with mean temperature $\bar{T}_1$, mean density $\bar{\rho}_1$ and speed of sound $c_1$) and a hot region (with $\bar{T}_2$, $\bar{\rho}_2$ and $c_2$) using a steady heat source located at $x_q$.

## 2. The tailored Green's function

Green's function is defined as an impulsive response of a point source at position $x'$ and time $t'$ that is observed at position $x$ and time $t$. Its governing equation is

$$\frac{1}{c^2}\frac{\partial^2 G}{\partial t^2} - \frac{\partial^2 G}{\partial x^2} = \delta(x - x')\delta(t - t') \tag{1}$$

In this equation, $c$ is the speed of sound; the impulsive point source is described by the term $\delta(x - x')\delta(t - t')$, which represents a point source at position $x'$, discharging an impulse at time $t'$. The *tailored* Green's function is the impulse response in a bounded space, i.e. an acoustic resonator, and it is therefore a superposition of resonator modes, which can be written as

$$G(x, x', t, t') = H(t - t')\, Re \sum_{n=1}^{\infty} g_n(x, x') e^{-i\omega_n (t-t')} \tag{2}$$

$g_n$ *and* $\omega_n$ can be calculated analytically for tubes with uncomplicated geometries. Details of such calculations can be found in[1]. The set-up considered in this paper is shown in Figure 1.

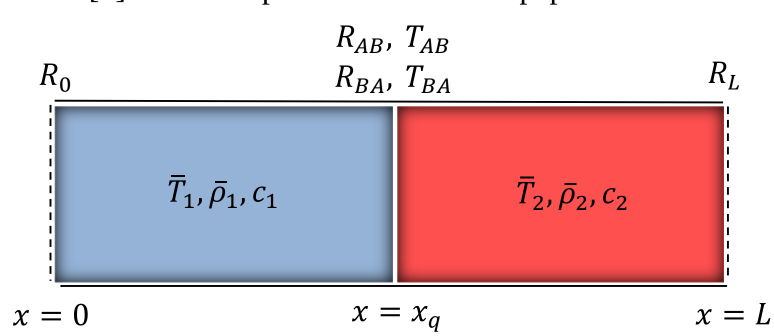


Figure 1: The set up with an interface between cold and hot region.

The interface at $x_q$ is described by the reflection and transmission coefficients $R_{AB}$, $R_{BA}$, $T_{AB}$ and $T_{BA}$. $R_0$ and $R_L$ are reflection coefficients at inlet and outlet of the tube. The characteristic equation to obtain modal frequencies of the Green's function for this set-up is $F(\omega) = 0$, where

$$F(\omega) = e^{-ik_1x_q}\, e^{ik_2(x_q-L)} - R_{BA}R_L e^{-ik_1x_q}\, e^{-ik_2(x_q-L)} - R_0R_{AB}e^{ik_1x_q}\, e^{ik_2(x_q-L)} + R_0R_L e^{ik_1x_q}\, e^{-ik_2(x_q-L)}\,(R_{AB}R_{BA} - T_{AB}T_{BA}) \tag{3}$$

In order to solve this, we use root finding methods (e.g. Newton Raphson method).

The modal amplitudes of the Green's function are given by

$$g_n(x,x') = \frac{c_2\,\hat{g}(x,x',\omega)}{2\omega_n\,F'(\omega_n)} \tag{4}$$

where

$$\hat{g}(x,x',\omega) = \begin{cases} A(x,\omega)B(x',\omega) & 0 < x < x_q \\ B(x',\omega)C(x,\omega) & x_q < x < x' \\ C(x',\omega)B(x,\omega) & x' < x < L \end{cases} \tag{5}$$

$$A(x,\omega) = T_{BA}(R_0e^{ik_1x} + e^{-ik_1x}) \tag{6}$$

$$B(x,\omega) = e^{ik_2(x-L)} + R_Le^{-ik_2(x-L)} \tag{7}$$

$$C(x,\omega) = e^{ik_2(x-x_q)}\left(R_{BA}e^{-ik_1x_q} + R_0e^{ik_1x_q}\right) + e^{-ik_2(x-x_q)}(e^{-ik_1x_q} - R_{AB}R_0e^{ik_1x_q}) \tag{8}$$

# 3. Green's function approach including noise

We base our Green's function approach on the acoustic analogy equation for the velocity potential $\phi(x,t)$

$$\frac{1}{c^2}\frac{\partial^2\phi}{\partial t^2} - \frac{\partial^2\phi}{\partial x^2} = -\frac{\gamma-1}{c^2}q(x,t) + F_n(x,t) \tag{9}$$

This has two source terms: the first represents the heat source with heat release rate $q(x,t)$, and the second source term, $F_n(x,t)$, represents random external noise. For the initial conditions, we assume

$$\phi(x,0) = \phi_0\delta(x-x_q), \qquad \frac{\partial\phi(x,0)}{\partial t} = \phi_0'\delta(x-x_q) \tag{10}$$

We describe the heat release rate distribution by $q(x,t) = q(t)\delta(x-x_q)$, which represents a compact heat source at $x = x_q$. For $q(t)$, we use (see [2])

$$q(t) = K\left[n_1u_q(t-\tau) - n_0u_q(t)\right] \tag{11}$$

where $K, n_1, n_0$ and $\tau$ are defined as

$$K = \frac{\bar{Q}}{\bar{U}s\bar{\rho}} \tag{12}$$

$$n_1 = \frac{g_{max}(A)+1}{2}, n_0 = \frac{g_{max}(A)-1}{2} \tag{13}$$

$$g_{max} = g_0 - g_1\left(\frac{A}{\bar{U}}\right) \tag{14}$$

$$\tau = \tau_0 + \tau_2\left(\frac{A}{\bar{U}}\right)^2 \tag{15}$$

The Green's function approach involves a series of mathematical steps, where the acoustic analogy equation (9) is combined with the governing PDE (1) for the Green's function, to give an integral equation for the acoustic velocity at the heat source (for details, see [1]). The end result is

$$u_q(t) = \frac{\partial \phi}{\partial x}_{x=x_q} = -\frac{\gamma-1}{c^2}\int_{t'=0}^{t} \frac{\partial G(x,x',t,t')}{\partial x}_{\substack{x=x_q \\ x'=x_q}} q(t')\,dt' + \int_{t'=0}^{t} F_n(t')\frac{\partial G(x,x',t,t')}{\partial x}_{\substack{x=x_q \\ x'=x_q}} dt' - \frac{\phi_0}{c^2}\frac{\partial G}{\partial x \partial t'}_{\substack{x=x_q \\ x'=x_q \\ t'=0}} + \frac{\phi_0'}{c^2}\frac{\partial G}{\partial x}_{\substack{x=x_q \\ x'=x_q \\ t'=0}} \tag{16}$$

### 3.1 Time evolution

In order to calculate the time history of the system based on equation (16), a numerical iteration procedure is performed. To this end, we define the following integrals

$$I_n^q(t) = \int_{t'=0}^{t'=t} e^{i\omega_n t'} q(t')dt', \qquad I_n^N(t) = \int_{t'=0}^{t'=t} e^{i\omega_n t'} F_n(t')dt' \tag{17}$$

Splitting the integral interval into two parts ($t' = 0, \ldots t - \Delta t$ and $t' = t - \Delta t, \ldots, t$) turns the integrals in equation (17) to

$$I_n^q(t) = \int_{t'=0}^{t'=t-\Delta t} e^{i\omega_n t'} q(t')\,dt' + \int_{t'=\mathrm{t}-\Delta \mathrm{t}}^{t'=t} e^{i\omega_n t'} q(t')\,dt' \tag{18}$$

$$I_n^N(t) = \int_{t'=0}^{t'=t-\Delta t} e^{i\omega_n t'} F_n(t')\,dt' + \int_{t'=\mathrm{t}-\Delta \mathrm{t}}^{t'=t} e^{i\omega_n t'} F_n(t')\,dt' \tag{19}$$

Substituting equations (17-19) and $G(x, x', t, t')$ from equation (2) into equation (16) leads to

$$u_q(t) = -\frac{\gamma-1}{c^2} Re \sum_{n=1}^{\infty} G_n e^{-i\omega_n t} I_n^q(t) + \sum_{n=1}^{\infty} G_n e^{-i\omega_n t} I_n^N(t) - \frac{1}{c^2} Re \sum_{n=1}^{\infty} (i\omega_n \varphi_0 + \varphi_0') G_n e^{-i\omega_n t} \tag{20}$$

where

$$G_n = \frac{\partial g_n(x,x')}{\partial x} \tag{21}$$

$$I_n^q(t) = I_n^q(t-\Delta t) + q(t-\Delta t)\frac{1 - e^{i\omega_n \Delta t}}{i\omega_n} e^{i\omega_n t} \tag{22}$$

$$I_n^N(t) = I_n^N(t-\Delta t) + F_n(t-\Delta t)\frac{1 - e^{i\omega_n \Delta t}}{i\omega_n} e^{i\omega_n t} \tag{23}$$

## 4. Validation

In order to validate equation (19), we assume that there is no random noise in the system, i.e. $F_n(t) = 0$), and use the stability predictions in [2] as a benchmark. These are reproduced in Figure 2 in the form of a stability map with heat source position $x_q$ as bifurcation parameter; $A/\overline{U}$ is defined as non-dimensional velocity amplitude of the acoustic field.

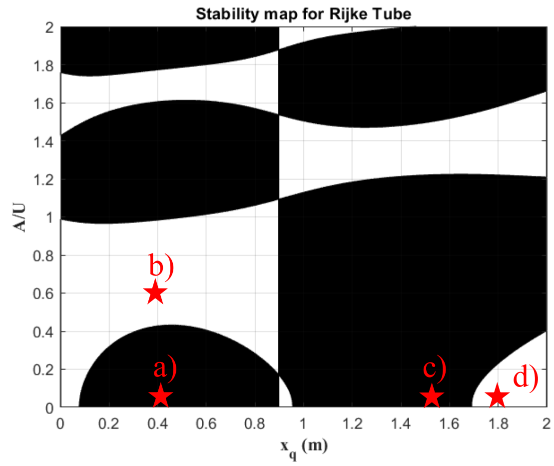


Figure 2: Stability map for a Rijke tube with temperature jump; white regions indicate stability, while black regions indicate instability**.** The following parameter values were used:

$$g_0 = 1.4, g_1 = 0.3, \tau_0 = 5 \times 10^{-3}\text{s},\ \tau_2 = 4.4 \times 10^{-3}\text{s}, \overline{T_1} = 304\ K,\ \overline{T}_2 = 460\ K, L = 2\ m, K = 3 \times 10^5\ W\ s\ kg^{-1}$$

The black regions show the unstable regions and white regions are stable regions. The amplitude-dependent time-lag is the reason for the appearance of stable and unstable region with increasing $A/\overline{U}$.

We calculated the time histories for four points in this stability map as described in section 3.1. The results are shown in Figure 3. The values of $g_0, g_1, \tau_0$ and $\tau_2$ in the heat release rate model are constant, and their values are given by $g_0 = 1.4, g_1 = 0.3, \tau_0 = 5 \times 10^{-3}\text{s}$ and $\tau_2 = 4.4 \times 10^{-3}\text{s}$. The temperature jump is from $\overline{T_1} = 304\ K$ to $\overline{T}_2 = 460\ K$. The length of tube and heater power are $L = 2\ m$ and $K = 3 \times 10^5\ W\ s\ kg^{-1}$, respectively. All these parameters correspond to those for Figure 2.

Point ($x_q = 0.4\text{m}, A/\overline{U} = 0.01$) is unstable in the stability map, so we expect to observe an exponential growth, followed by a limit cycle with an amplitude around 0.44. Figure 3a shows an exponential growth until about $x_q$=0.12m, and a limit cycle with amplitude 0.44 beyond about $x_q$=0.17m; this is in complete agreement with the stability map in Figure 2. Point ($x_q = 0.4\text{m}, A/\overline{U} = 0.6$) which is in the stable region in the stability map shows an initial decay in amplitude, and quickly reaches a stable limit cycle, again with amplitude 0.44; this is shown in Figure 3b. Again, this is fully in line with the results in the stability map.

For point ($x_q = 1.5\text{m}, A/\overline{U} = 0.01$), which is in the unstable region but in the downstream side of the tube, the time history in Figure 3c shows a an initial growth, followed by a limit cycle with amplitude around 1.2. The stability map for this point confirms the result. Finally, for a point in stable region ($x_q = 1.8\text{m}, A/\overline{U} = 0.01$) we expect the amplitude to decay to zero. Figure 3d validates the result in the stability map. Now that we have successfully validated our approach, we will perform the same calculations, but include random noise, and study effect of the noise on the stability of the system.

a)

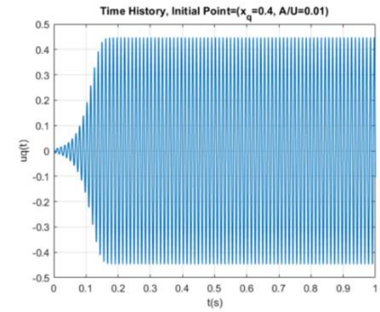


b)

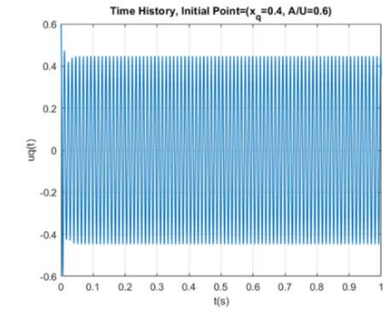


c)

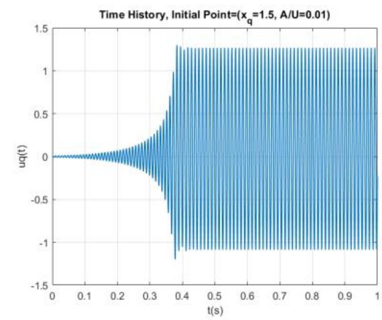


d)

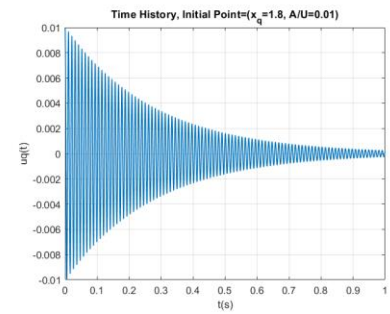


Figure 3: Time history of the Rijke tube. (a) Point $(\mathrm{x_q} = 0.4\mathrm{m}, \mathrm{A}/\overline{\mathrm{U}} = 0.01)$ (b) Point $(\mathrm{x_q} = 0.4\mathrm{m}, \mathrm{A}/\overline{\mathrm{U}} = 0.6)$ (c) Point $(\mathrm{x_q} = 1.5\mathrm{m}, \mathrm{A}/\overline{\mathrm{U}} = 0.01)$ (d) Point $(\mathrm{x_q} = 1.8\mathrm{m}, \mathrm{A}/\overline{\mathrm{U}} = 0.01)$

## 5. Time evolution results in the presence of noise

We will now calculate the time history for the two points in Figure 3a and 3c, with noise present. The level of the noise is described by the parameter β, which can take values 1 (small), 2 (medium) and 4 (high). The blue curves in Figure 4a,b,c show the time evolution for point $(x_q = 0.4\mathrm{m}, \mathrm{A}/\overline{\mathrm{U}} = 0.01)$, which is in the unstable region, for β=1,2,4. For comparison, the equivalent curves for the noiseless case have been added in red. Figure 4a shows that a low level of noise ($\beta = 1$) has a small effect on the stability behaviour. If the noise level is increased, the time it takes for the limit cycle to develop becomes shorter (see Figures 4b,c). Figures 5a,b,c show the same behaviour for the point $(x_q = 1.5m, A/\overline{U} = 0.01)$. This phenomenon is already known from experimental observations [4]. Both Figures 4 and 5 show that the amplitude of the limit cycle does not change significantly with increasing noise level. This is partly, but not fully, in agreement with the predictions by Waugh and Juniper [6].

a)

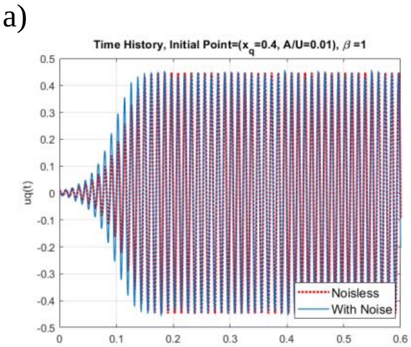


b)

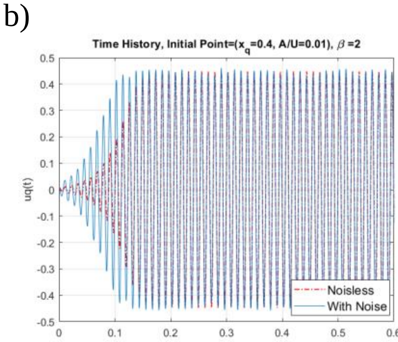


c)

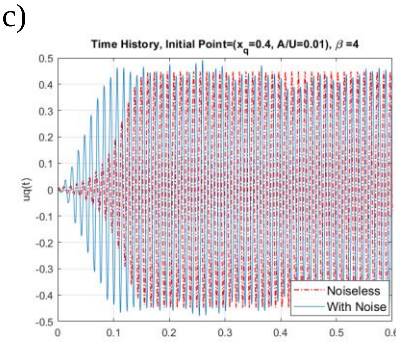


Figure 4: Time evolution for point $(x_q = 0.4, \mathrm{A}/\overline{\mathrm{U}} = 0.01)$ for different levels of noise

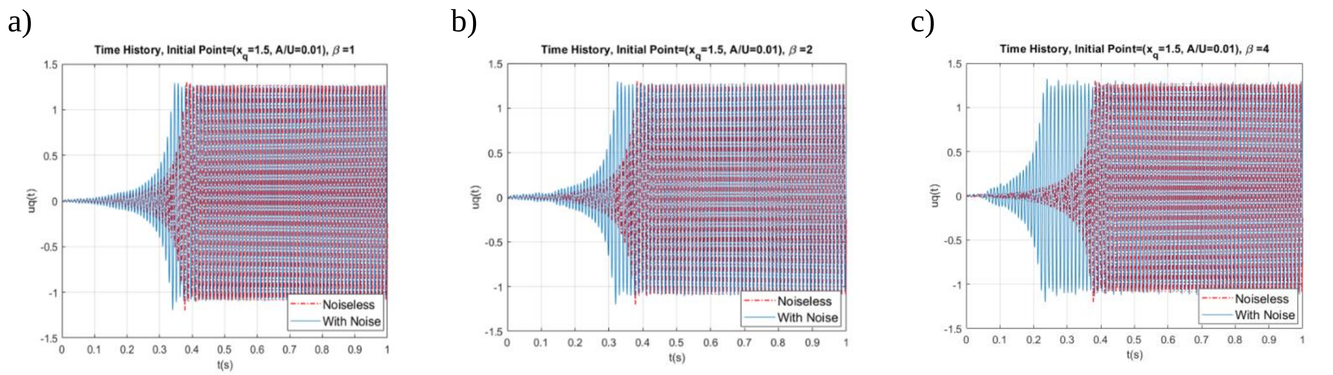


Figure 5: Time evolution for point ($x_q = 1.5, A/\overline{U} = 0.01$) for different levels of noise

In addition, we have chosen the point ($x_q = 1.8, A/\overline{U} = 0.2$) to investigate the effects of noise. This point is located in the *stable* region, but close to its upper boundary. In this case, an increase in the noise level leads to a dramatic change in the stability behaviour (see Fig. 6). For β=1 (Fig. 6a), the oscillation amplitude decreases fairly steadily; after that the noise becomes noticeable, but has no effect on the stability behaviour. A similar trend can be seen for β=2, 4 (Fig. 6b,c), except that the amplitude decay is more irregular. Figure 6d, which is for β=8, shows a very different scenario: the amplitude decay has been replaced by an amplitude *increase*, which continues until about *t*=0.4s, and then a limit cycle develops. The amplitude of this limit cycle is about 1.2, which is close to the upper edge of the region of instability above the point $x_q = 1.8$. This phenomenon is known as triggering [4]

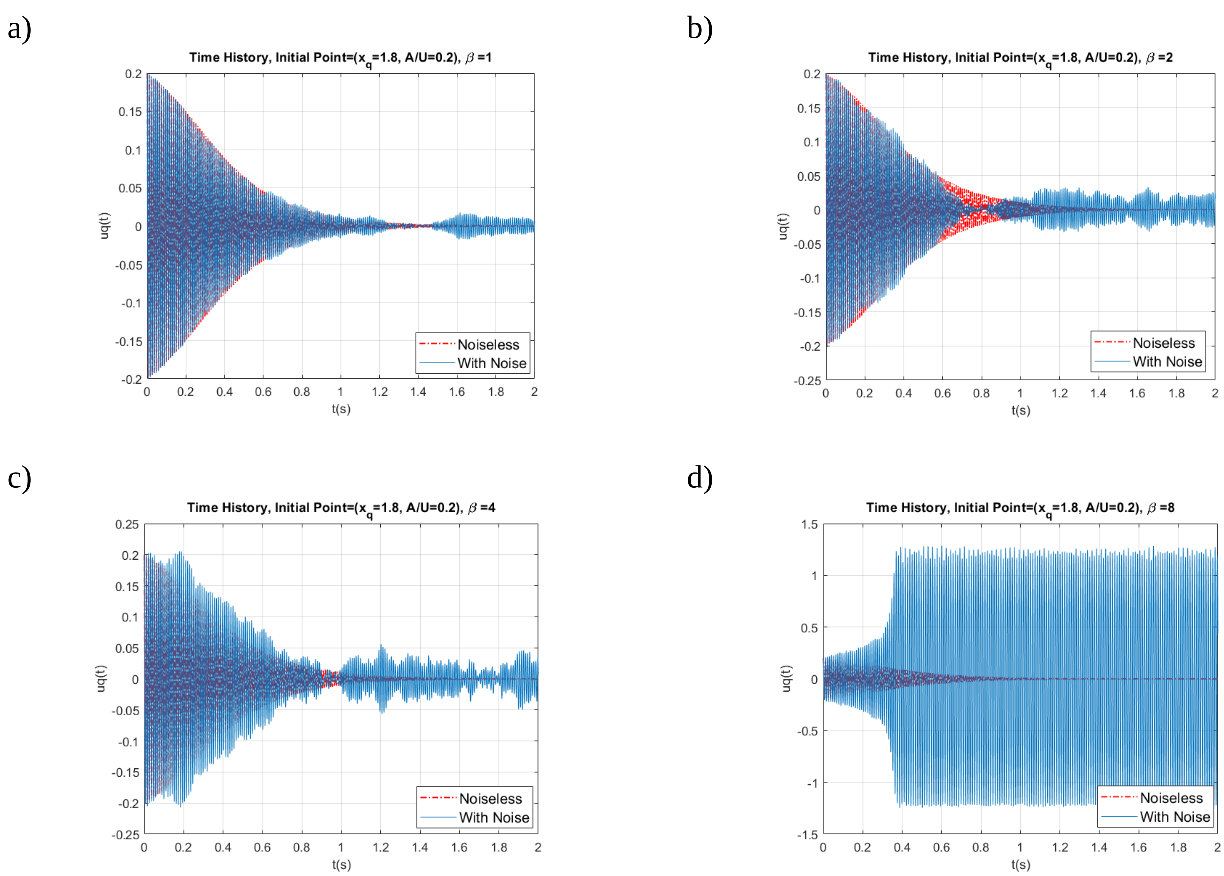


Figure 6: Time evolution for point ($x_q = 1.8, A/\overline{U} = 0.2$) for different levels of noise

## 6. Conclusion

In this paper, we investigated the effects of noise on a thermoacoustic system. An extended Green's function approach was established; this includes two forcing terms: one to describe the heat release rate (this is coupled nonlinearly to the acoustic field), and one to describe the noise (this has a variable level and is independent of the acoustic field). We validated our method by comparing our predictions for the noiseless case with earlier results obtained from a modal analysis approach. There was excellent agreement for the stability behaviour as well as for the limit cycle amplitudes. Next, we performed calculations of the time evolution including random noise, and we made the following predictions. (1) Increasing the level of noise can change the stability behaviour of the system. This means that the noise can trigger an instability in a thermoacoustic system that would be stable if noise was absent. Indeed, the level of the noise plays an important role in the stability behaviour. (2) The noise can make the transient time, i.e. the time it takes for a limit cycle to establish, faster. Once a limit cycle is established, its amplitude is barely affected by the noise; in fact, it is almost the same for the system with or without noise. All our predictions are in line with experimental observations.

Our Green's function approach gives fast predictions and is very versatile. We will use it to shed further light on nonlinear thermoacoustic systems; in particular, we will perform a comprehensive investigation of the influence of noise.

## 7. Acknowledgement

This work is part of the Marie Skłodowska-Curie Initial Training Network **Pol**lution **K**now-How and **A**batement (POLKA). We gratefully acknowledge the financial support from the European Commission under call H2020-MSCA-ITN-2018**.**

## REFERENCE

[1] M. A. Heckl, "Analytical model of nonlinear thermo-acoustic effects in a matrix burner," *J. Sound Vib.*, vol. 332, no. 17, pp. 4021–4036, 2013.

[2] N. Noiray, "Linear and nonlinear analysis of combustion instabilities, application to multipoint injection systems and control strategies," Ecole Centrale Paris, 2007.

[3] A. Bigongiari and M. A. Heckl, "A Green's function approach to the rapid prediction of thermoacoustic instabilities in combustors," pp. 970–996, 2016.

[4] V. Jegadeesan and R. I. Sujith, "Experimental investigation of noise induced triggering in thermoacoustic systems," *Proc. Combust. Inst.*, vol. 34, no. 2, pp. 3175–3183, 2013.

[5] M. A. Heckl, "Analytical model of nonlinear thermo-acoustic effects in a matrix burner," *J. Sound Vib.*, vol. 332, no. 17, pp. 4021–4036, 2013.

[6] I. C. Waugh and M. P. Juniper, "Triggering in a thermoacoustic system with stochastic noise," *Int. J. spray Combust. Dyn.*, vol. 3, no. 3, pp. 225–241, 2011.